


**Depinning of Driven Systems:
Time-resolved x-ray scattering measurements of the
charge-density waves in NbSe₃**

Joel D. Brock
Professor and Director
School of Applied & Engineering Physics

Director
*G-line Division, Cornell High Energy Synchrotron Source (CHESS)
Cornell University, Ithaca, NY*

 1

Brock Research Group KITP August 19, 2003



Acknowledgements

Kristin Ringland¹, Robin Sampson, Jun-Dar Su, and Yanping Li²
*School of Applied & Engineering Physics
Cornell University, Ithaca, NY 14853*

S.G. Lemay³, and R.E. Thorne
*Department of Physics
Cornell University, Ithaca, NY 14853*

Mark Sutton
*Department of Physics
McGill University, Montreal, CANADA*

1. McKinsey & Company, Stockholm, Sweden
2. Applied Materials Inc., Santa Clara, CA
3. Delft University of Technology, Delft, The Netherlands


 2

Brock Research Group KITP August 19, 2003

Outline

- Intro to CDW Physics/Phenomenology
- Intro to Modern X-ray Technology
- Properties of NbSe₃
- Experimental Details – Sample quality
- Kinetics of Relaxation from Sliding State
- Structure of the Sliding & Zero-field cooled States
- Low Temperature Phase Diagram
- Coherent X-ray Measurements: “Speckle”
- Summary

Brock Research Group KITP August 19, 2003
3

CDW Basics

In Quasi-One-Dimensional Metals...

- At $T=0$, Electronic energy is lowered by opening an energy gap at the Fermi surface.
- Periodic potential required to do this can be supplied by a longitudinal lattice-density wave (LDW).
- Elastic energy cost for LDW is less than electronic energy gain

$$\rho = \bar{\rho} + \Delta \cos(2k_F \hat{b} \cdot \vec{r} + \phi(\vec{r}))$$

$$\vec{u}(\vec{r}) = \vec{u}_0 \sin(2k_F \hat{b} \cdot \vec{r} + \phi(\vec{r}))$$

Brock Research Group KITP August 19, 2003
4

Sliding CDWs

Since the wavelength of a CDW is (usually) incommensurate with the periodicity of the lattice, there is no elastic restoring force. In an ideal crystal, the CDW can “slide” rigidly without friction.

Defects in the crystal lattice provide “friction,” creating a threshold field.

The graph shows the second derivative of the intensity, d^2rdi [arb], plotted against the electric field in mV/cm . The data is taken at $120K$. A vertical dashed line marks the threshold field E_T at approximately 100 mV/cm . For fields below E_T , the signal is constant at a high value. At E_T , there is a sharp drop, and for fields above E_T , the signal decreases more gradually, following a curve that levels off at higher field values.

Brock Research Group KITP August 19, 2003
5

General Predictions

- At zero field, periodicity of lattice → quasi long-range translational order
- Far below threshold: thermal activation → creep
- Topological defects → plastic flow
- Near elastic depinning threshold: similar to standard critical phenomena (velocity is order parameter).
- Far above threshold: recovery of perfect lattice

The phase diagram plots temperature T on the vertical axis and electric field E on the horizontal axis. A critical temperature T_c is marked on the vertical axis. The diagram is divided into four regions: 'fluid flow' (top right), 'plastic flow' (middle), 'creep' (bottom left), and 'moving solid' (bottom right). A curve labeled $E_c(T)$ separates the 'plastic flow' and 'moving solid' regions. Hashed lines indicate possible sharp crossovers between the 'fluid flow' and 'plastic flow' regions, and between the 'plastic flow' and 'creep' regions.

FIG. 1. Schematic phase diagram for the three-dimensional CDW. Hashed lines indicate (possible sharp) crossovers.
L. Balents and M.P.A. Fisher, PRL, 75, 4270 (1995)

Brock Research Group KITP August 19, 2003
6

X-ray scattering is nearly ideal probe

- non-perturbative
- direct interpretation
- structural measurement

$$S(\vec{q}, t) = \frac{1}{\Omega} |J_1(\vec{q} \cdot \vec{u}_0)|^2 \int_{\Omega} e^{i[(\vec{G} \pm 2k_F \hat{b}) - \vec{q}] \cdot \vec{r}} \overline{\langle e^{i\phi(\vec{r}, t)} e^{-i\phi(\vec{0}, t)} \rangle} d\vec{r}$$

$$\overline{\langle e^{i\phi(x, t)} e^{-i\phi(0, t)} \rangle} = e^{-\frac{1}{2}g(x, t)} \approx e^{-\frac{1}{2}([\phi(x, t) - \phi(0, t)]^2)}$$

Brock Research Group KITP August 19, 2003
7

Synchrotron Radiation

Radiation Cone

Electron orbit

Radius, R
($2\pi R \sim 750$ m)

$1/\gamma$

Dipole radiation pattern of accelerated charges is "folded" forward by special relativity, producing "search light" radiation pattern.

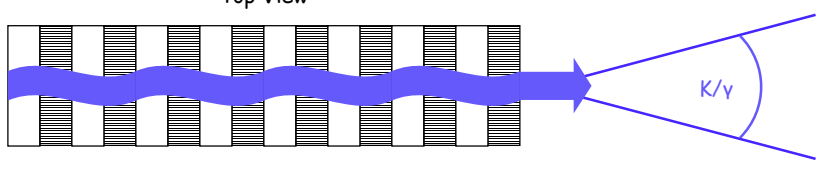
Characteristic opening angle is given by

$$\gamma^{-1} = (E/mc^2)^{-1} \sim 10^{-4} \sim 0.1 \text{ mrad}$$

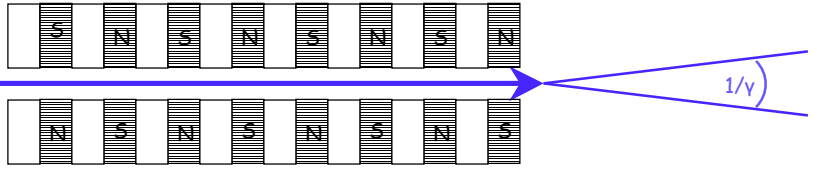
Brock Research Group KITP August 19, 2003
8

Increase Power with Wiggler Source


Top View



Side View



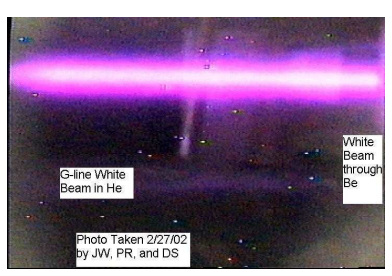
Brock Research Group KITP August 19, 2003

 9

Why bother?


At comparable energy and angular resolution...

- Rotating anode generator: $\sim 10^7$ x-rays/second
- Synchrotron source: $10^{12} - 10^{15}$ x-rays/second





Not your father's x-ray source!


Brock Research Group KITP August 19, 2003


 10


X-ray Synchrotron Sources

















Brock Research Group KITP August 19, 2003 11

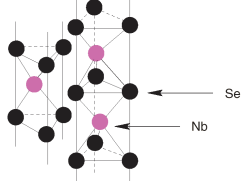
NbSe₃ Properties

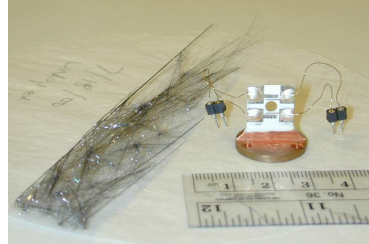
- monoclinic unit cell


$$\begin{aligned}
 a &= 10.009 \text{ \AA} \\
 b &= 3.4805 \text{ \AA} \quad \beta = 109.47 \\
 c &= 15.629 \text{ \AA}
 \end{aligned}$$

Hodeau *et al.*, J. Phys. C **11**, 4117 (1978)

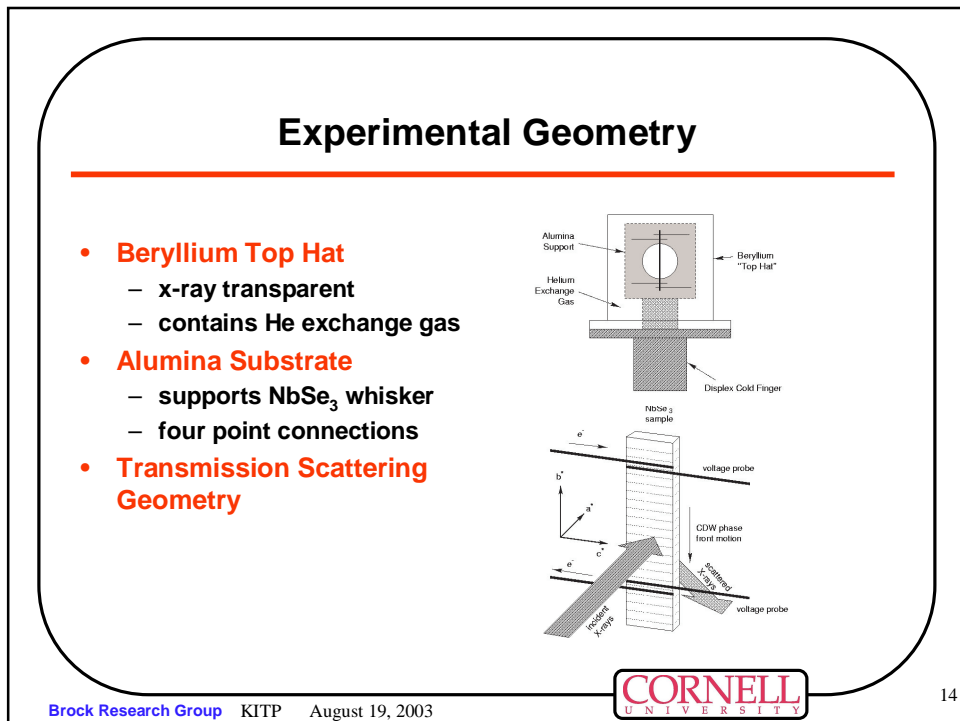
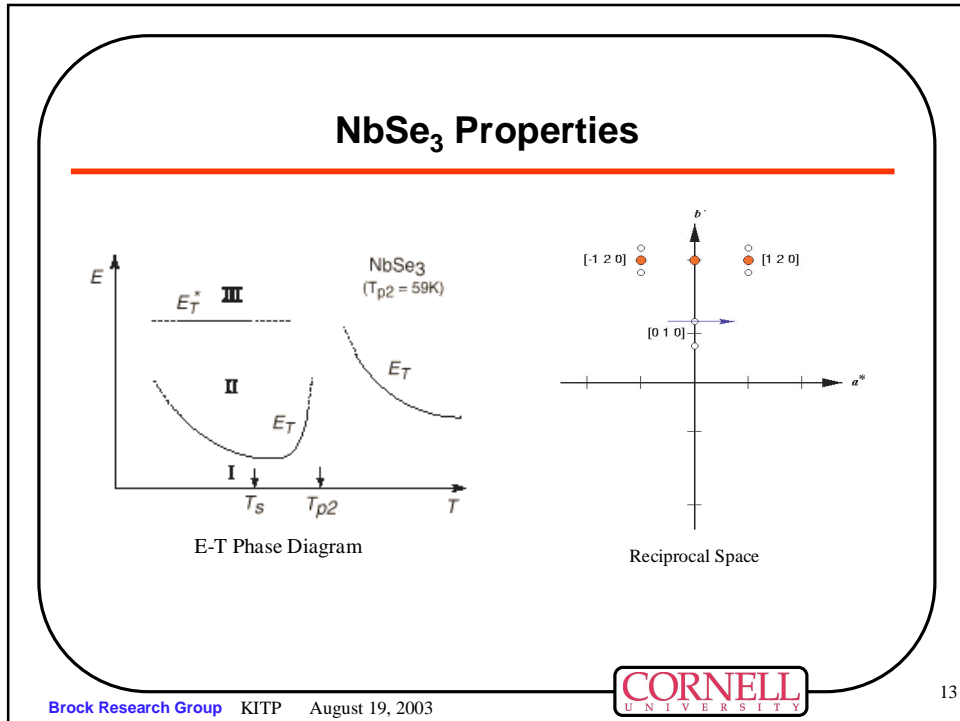
- whisker axis || to **b**, **b'**
- width || **c**
- thickness || **a'**
- $T_{P1} \approx 145 \text{ K}$, $T_{P2} \approx 59 \text{ K}$
- $Q_1 \approx (0 \ 0.243 \ 0)$
- $Q_2 \approx (0.5 \ 0.26 \ 0.5)$



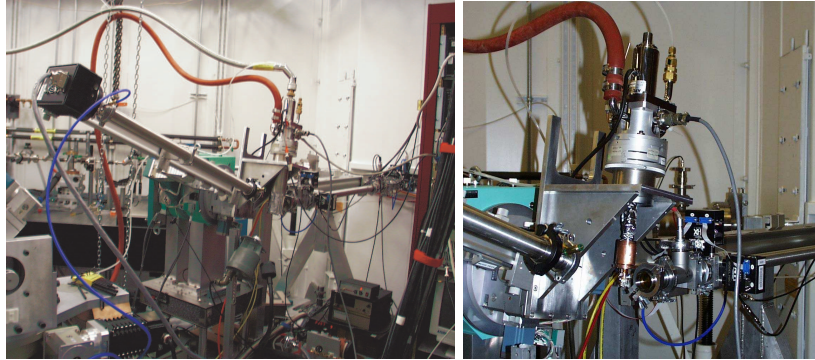




Brock Research Group KITP August 19, 2003 12



Experimental Geometry



Brock Research Group KITP August 19, 2003

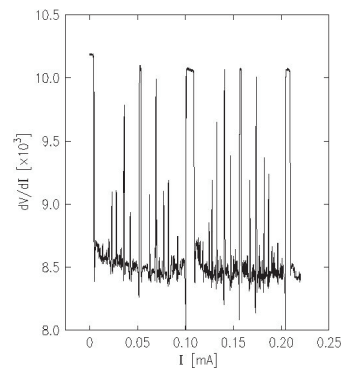


15

Sample Characterization

To study 'intrinsic' CDW properties, we need to make sure that there are no sample defects that might create extrinsic effects. Therefore, the criteria for choosing samples are:

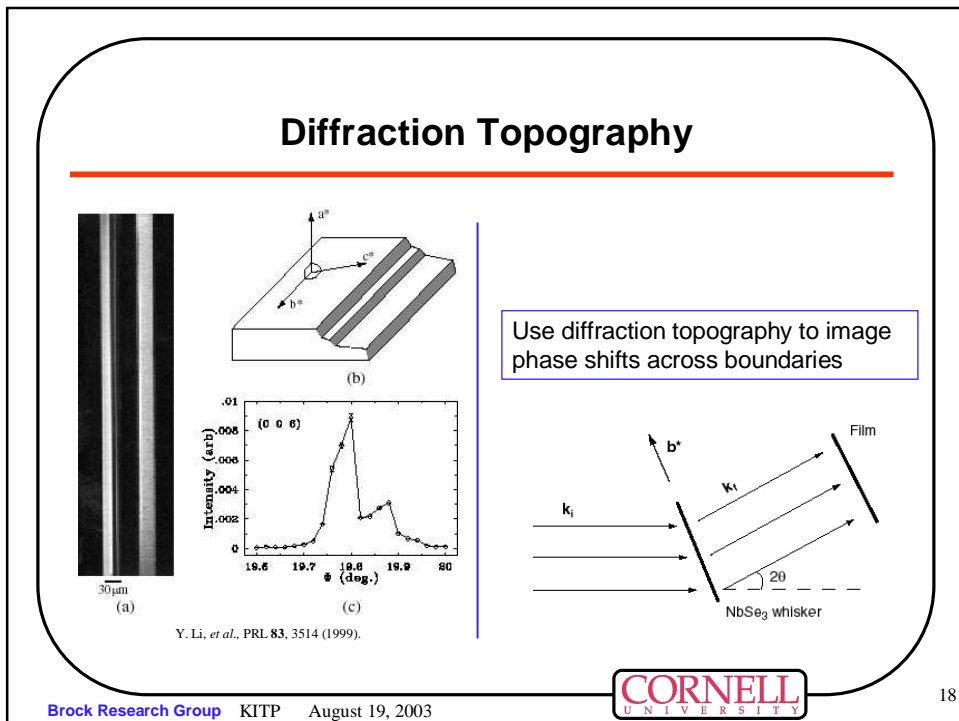
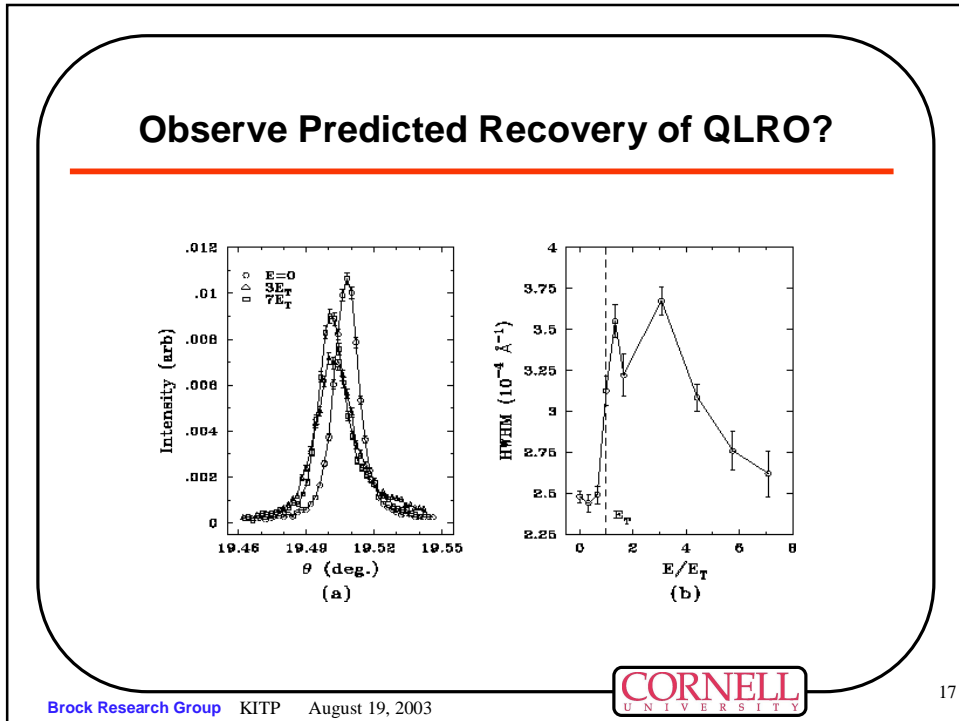
- Very regular cross sections
- Darwin limited (020) Bragg peaks
- Excellent mode-locking characteristics



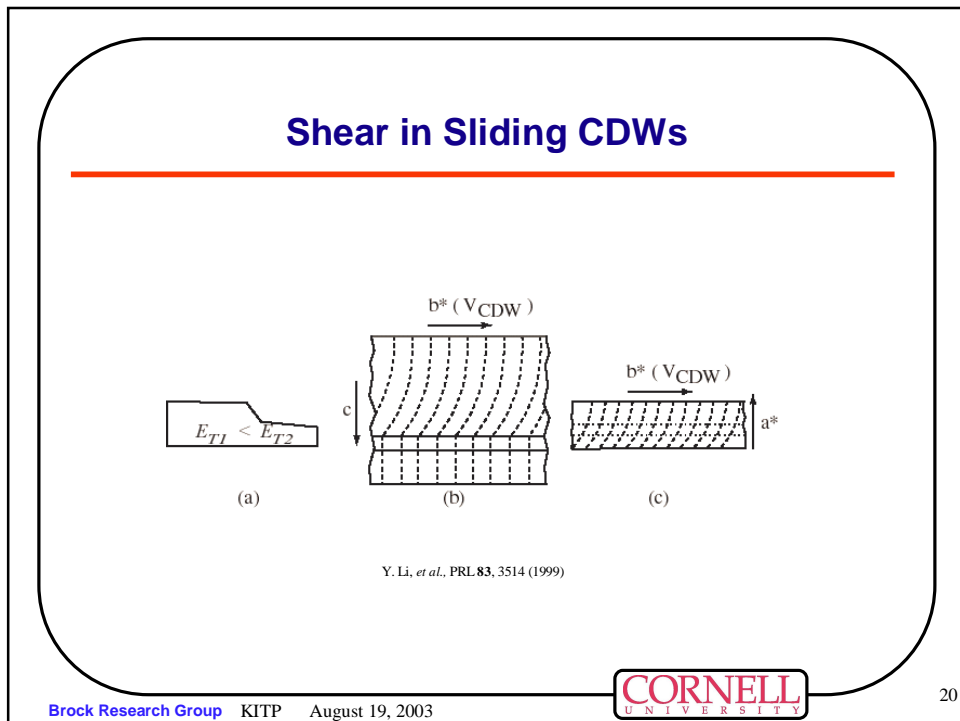
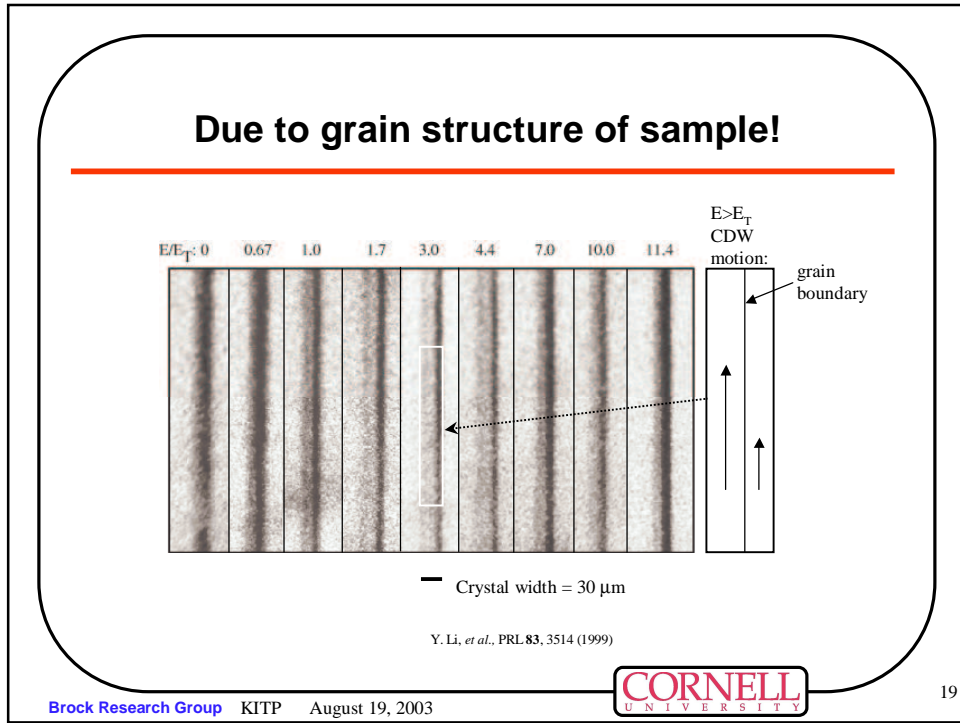
Brock Research Group KITP August 19, 2003



16




Depinning of Driven Systems: Time-resolved x-ray scattering measurements of the charge-density waves in NbSe3



Time-resolved Experiments

Weak scattering signal requires signal averaging or time-periodic signal.

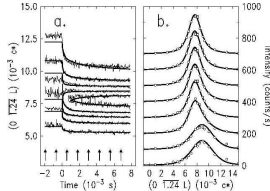
Brock Research Group KITP August 19, 2003

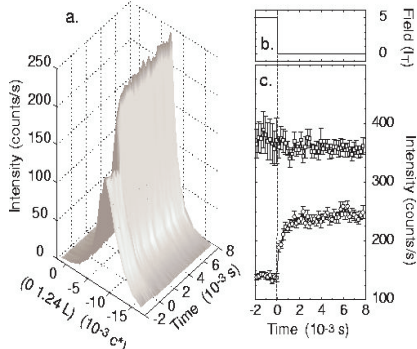


21

“Typical” Pinning Data


- Current is on for $t < 0$
- Current is off for $t > 0$
- CDW satellite responds by
 - sharpening
 - (possibly) small rotation
 - integrated intensity remains constant





K.L. Ringland *et al.*, PRL **82**(9), 1923-26 (1999).

Brock Research Group KITP August 19, 2003



22

Fukuyama-Lee-Rice Theory

Microscopic Model (based on Fröhlich Hamiltonian)

- P.A. Lee, T.M. Rice and P.W. Andersen. "Conductivity from charge or spin density waves." Solid State Comm., **14**, 703 (1974).

Phase only approximation (FLR)

- H. Fukuyama. "Pinning in Peierls-Fröhlich state and conductivity." J. Phys. Soc. Japan, **41**(2), 513 (1976).
- H. Fukuyama and P.A. Lee. "Dynamics of charge density wave. I. Impurity pinning in a single chain." Phys. Rev. B, **17**(2), 535 (1978).
- P.A. Lee and T.M. Rice. "Electric field depinning of charge density waves." Phys. Rev. B, **19**(8), 3970 (1979).

$$\Psi(x) = \bar{\psi} e^{i\phi(z)}$$

$$H_{FLR}[\phi(\vec{r}, t)] = \int d\vec{r} \left\{ \frac{\kappa}{2} (\nabla\phi)^2 + \sum_i \rho_{cdw} V(\vec{r} - \vec{R}_i) \cos(\vec{Q} \cdot \vec{r} + \phi) - E\phi \right\}$$

Brock Research Group KITP August 19, 2003

23

Solution to Equation of Motion

- **Use FLR Hamiltonian**
- **Ignore thermal noise**
- **E=0**
- **Spatial Fourier transform**
- **Integrate EOM**
- **Assume δ -correlated, quenched random-field**
- **Integrate to obtain $g(r,t)$**

$$\partial_t \phi = D\nabla^2 \phi + V(\vec{r})$$

$$\langle |\tilde{\phi}(\vec{q}, t)|^2 \rangle = \langle |\tilde{\phi}(\vec{q}, 0)|^2 \rangle e^{-2q^2 D t} + \frac{\langle |\tilde{V}(\vec{q})|^2 \rangle}{D^2 q^4} (1 - e^{-q^2 D t})^2$$

$$g(\vec{r}, t) \equiv \int_{1/r}^{\infty} d^3 \vec{q} \langle |\tilde{\phi}(\vec{q}, t)|^2 \rangle$$

B. Jancovici, Phys. Rev. Lett., **19**, 20 (1967).

Brock Research Group KITP August 19, 2003

24

Approximate Form for $g(x,t)$

Numerical Integration of FLR Solution

Approximation to FLR Solution

$$g(x,t) \equiv \int_{1/x}^{\infty} d^3 \vec{k} \langle |\phi(\vec{k},t)|^2 \rangle$$

$$g(x,t) \equiv \begin{cases} x/\xi_i & \text{for } x/t^\mu \geq 1 \\ x/\xi_f & \text{for } x/t^\mu \leq 1 \end{cases}$$

Brock Research Group KITP August 19, 2003

25

Approximate form for $S(\vec{q},t)$

Piece-wise integration using approximate form for $g(x,t)$

$$S(\vec{q},t) \approx \int_0^{t^\mu} d^3 \vec{r} e^{i(\vec{G} \pm \vec{Q} - \vec{q}) \cdot \vec{r}} e^{-|\vec{r}|/\xi_f} + \int_{t^\mu}^{\infty} d^3 \vec{r} e^{i(\vec{G} \pm \vec{Q} - \vec{q}) \cdot \vec{r}} e^{-|\vec{r}|/\xi_i}$$
$$S(\vec{q},t) \approx \frac{\xi_f}{1 + \xi_f^2 (q_\perp - G_\perp)^2} \left[1 - e^{-(t/\tau)^{1/2}} \right] + \frac{\xi_i}{1 + \xi_i^2 (q_\perp - G_\perp)^2} e^{-(t/\tau)^{1/2}}$$

Brock Research Group KITP August 19, 2003

26

Approximate form for S(q,t)

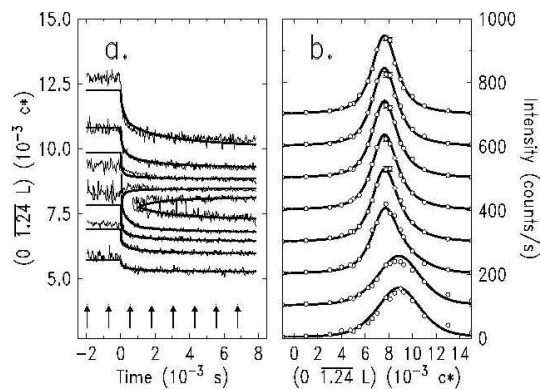
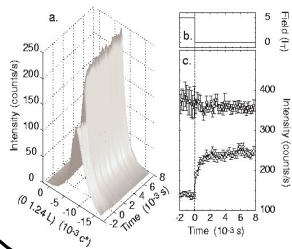
- $\mu \neq 1/2$, but keep $\alpha = 1/2$
- initial (sliding) state not Lorentzian
- integrate over broad directions of resolution function

$$S(q_{\perp}, t) \approx \frac{\xi_f}{1 + \xi_f^2 (q_{\perp} - G_{\perp})^2} \left[1 - e^{-(t/\tau)^{\mu}} \right] + S(q_{\perp}, t=0) e^{-(t/\tau)^{\mu}}$$

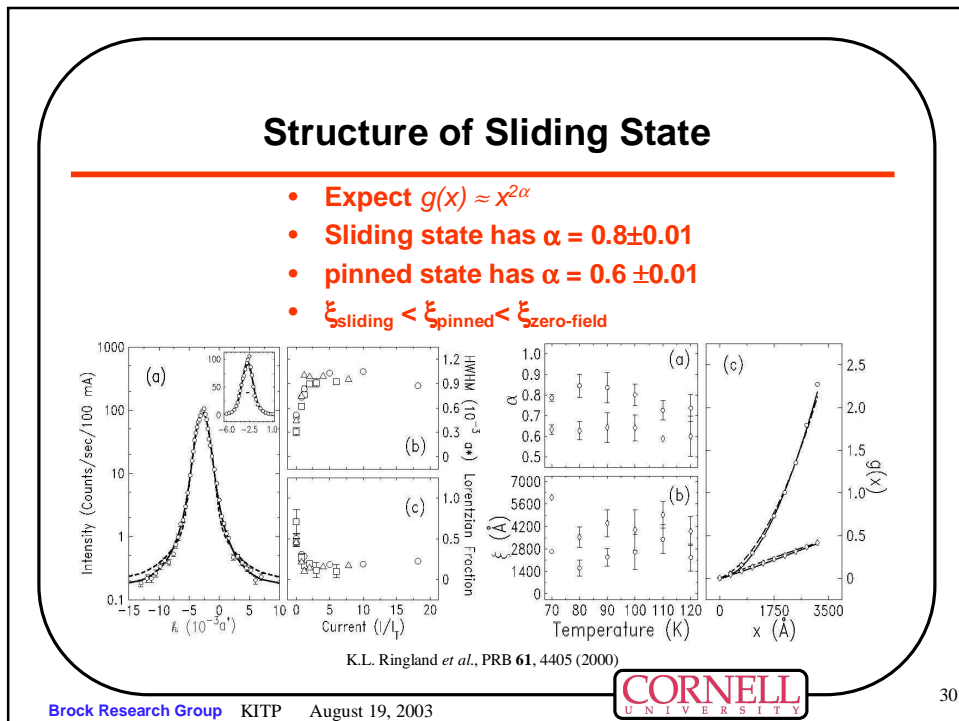
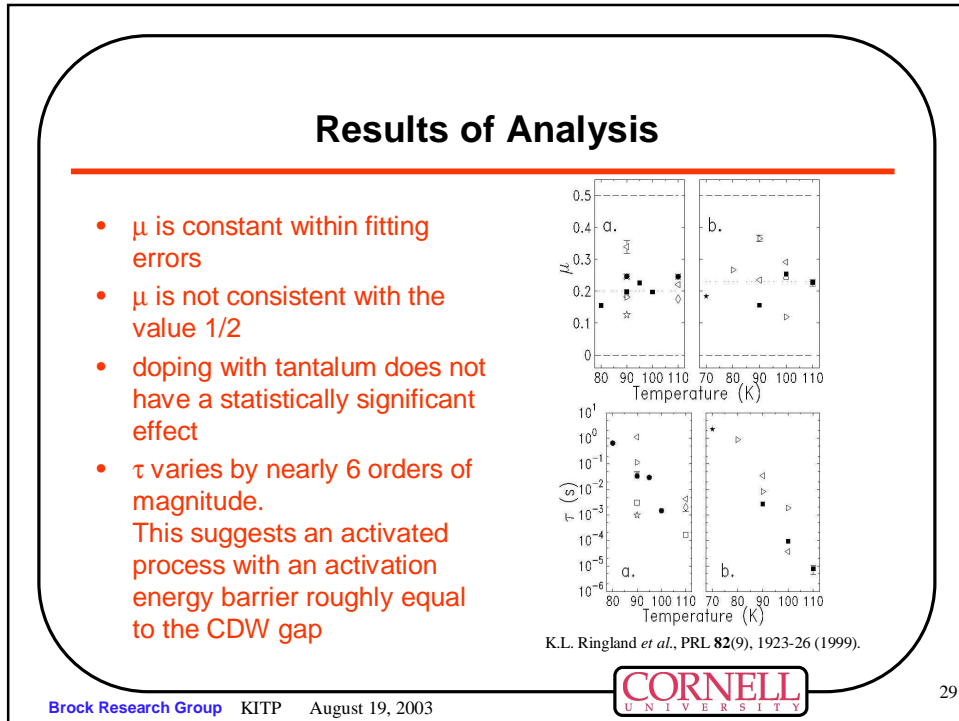
Simple "stretched exponential" kinetics

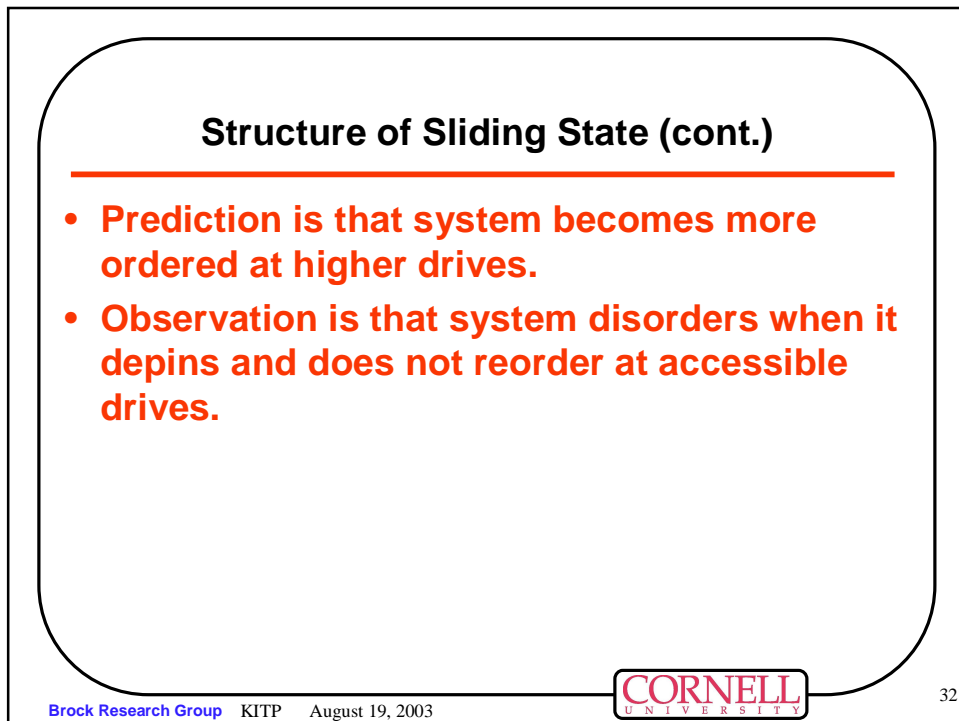
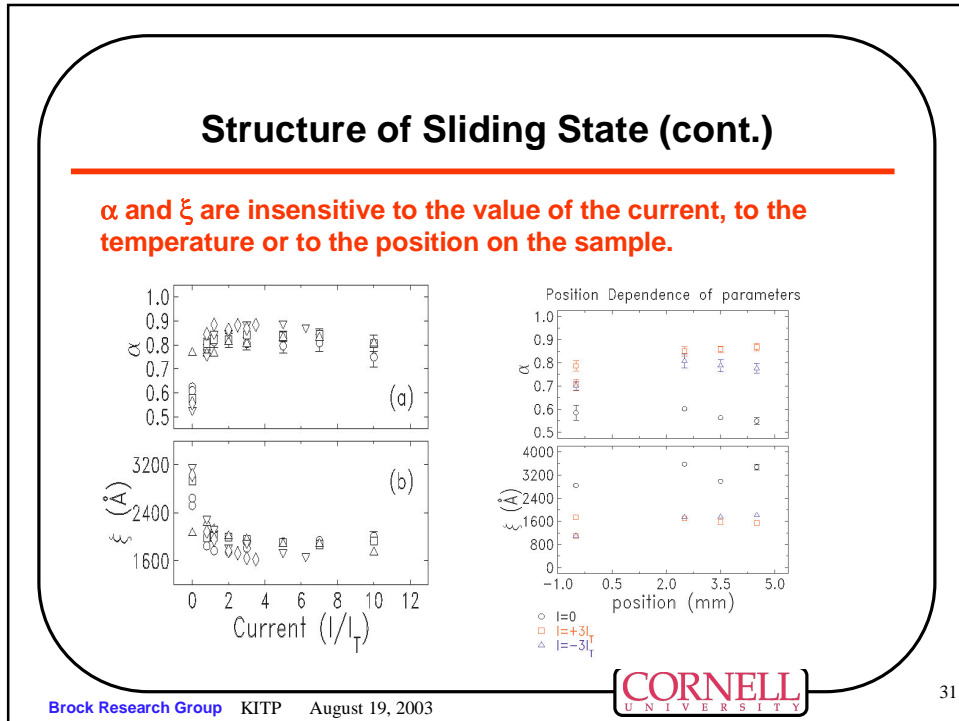
Results of Analysis

- Solid lines are best fit results using only data from $t > \tau$
- 2 parameter fit (μ and τ)
- $\chi^2 \approx 1.5$
- $\sim 2 \times 10^4$ degrees of freedom.
- Arrows indicate times for the "slices" depicted.



K.L. Ringland *et al.*, PRL **82**(9), 1923-26 (1999).





Relationship to Zero-Field Cooled State

- Zero-field Cooled
- New length scale required to describe short length scale behavior
- FLR Model is accurate

$$g(x) \cong \frac{\sqrt{a^2 + x^2} - a}{\xi}$$

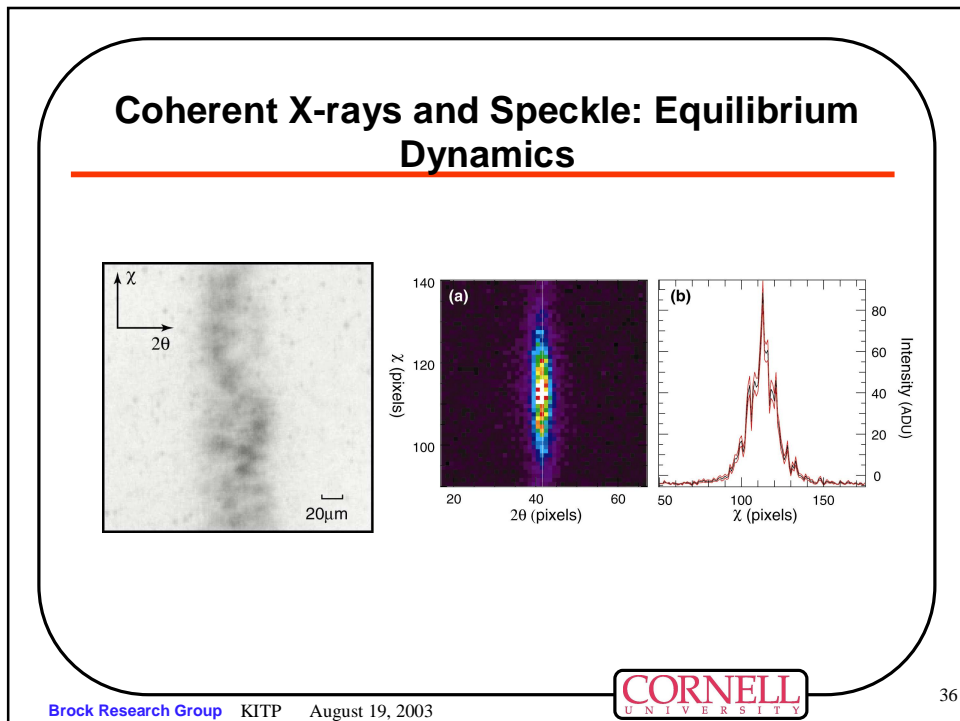
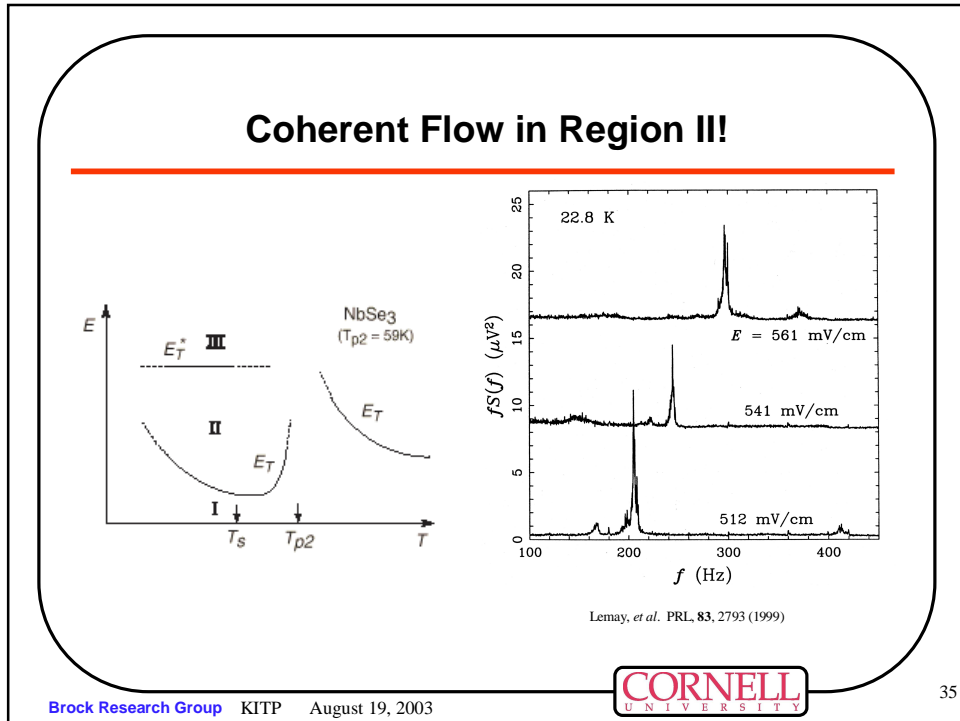
Brock *et al.*, PRL 73, 3588 (1994)

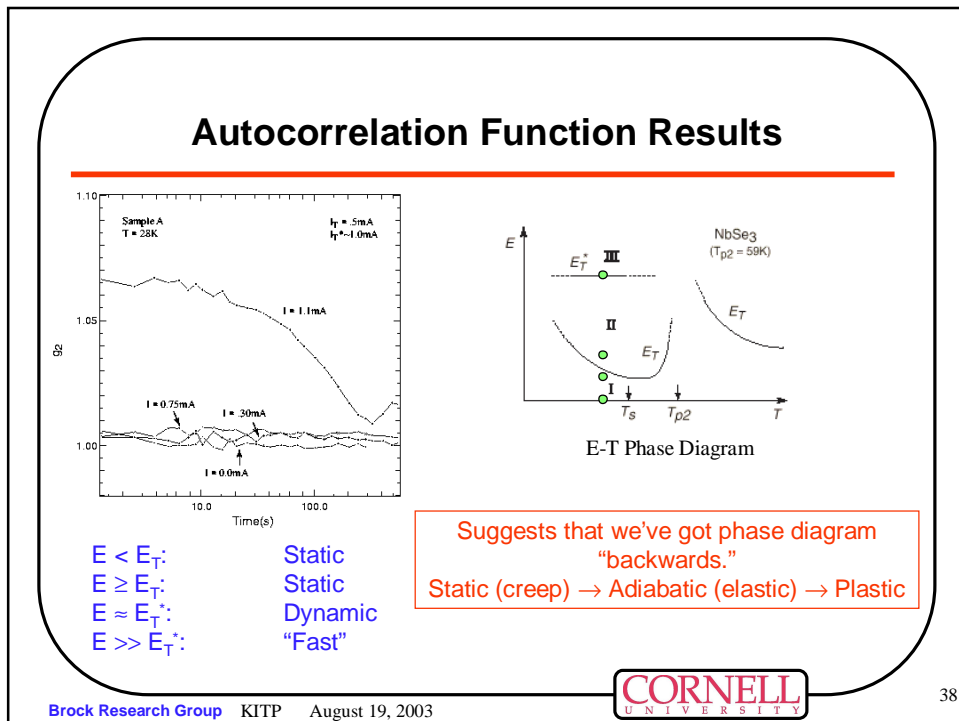
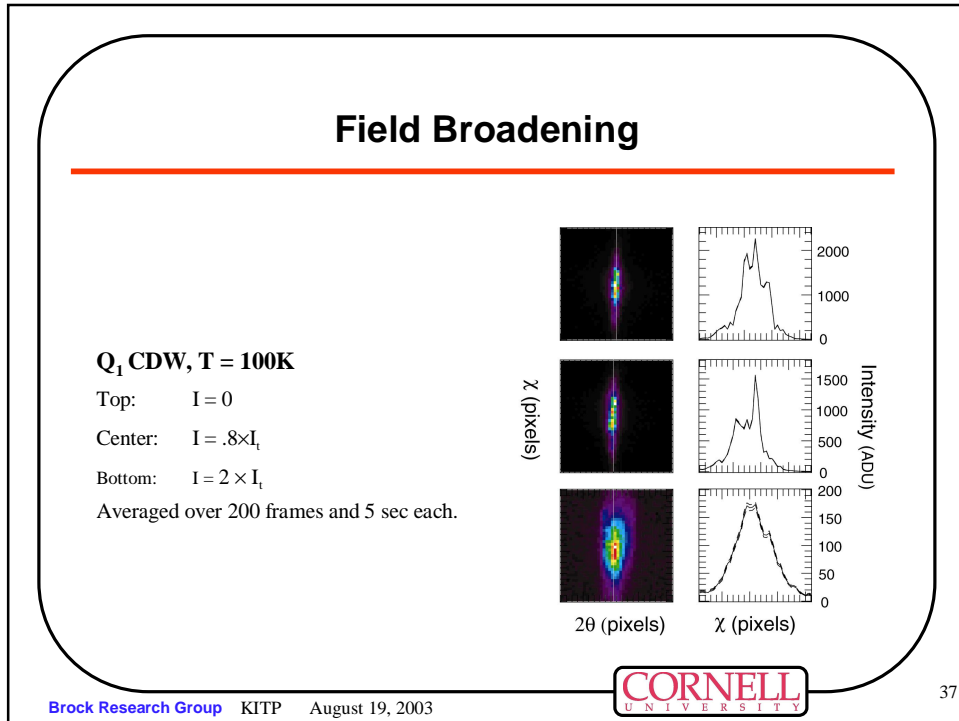
Brock Research Group KITP August 19, 2003
33

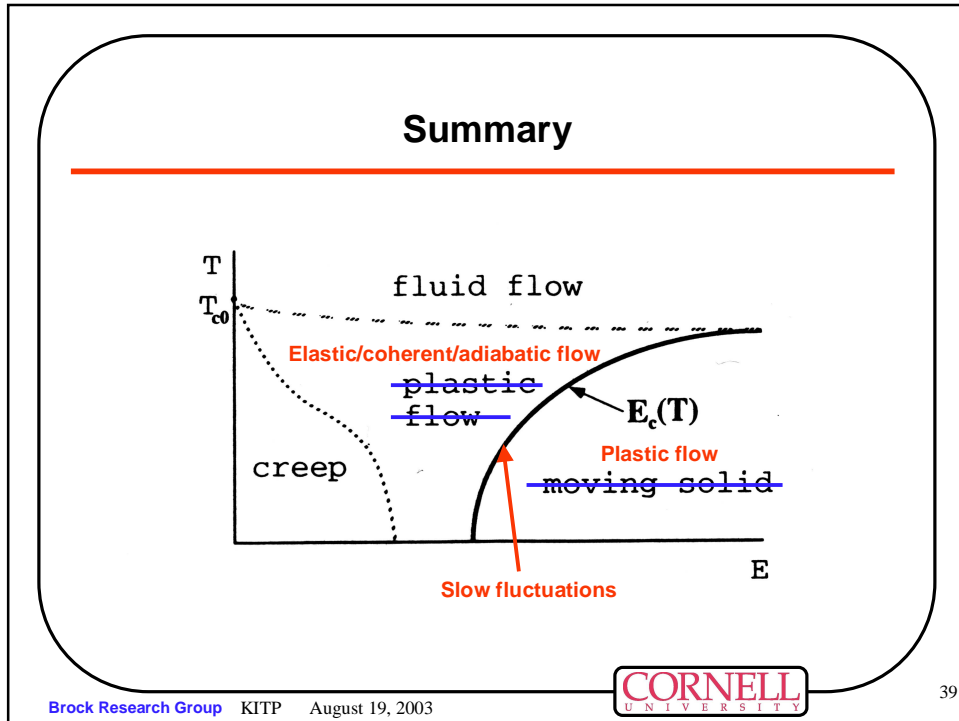
Low Temperature Behavior: Switching

NbSe₃
(Tp2 = 59K)

Brock Research Group KITP August 19, 2003
34







- ### So what should we do?
-
- **Need to expand our description of pinning/depinning**
 - **New models**
 - Amplitude fluctuations may be important
 - Elastic interactions may not be sufficient
 - **More data**
 - Nail down XPCS data
 - X-rays measures lattice-distortion wave. Transport measures conduction electron density wave.
- 40
- Brock Research Group KITP August 19, 2003
-

Viscoelastic Coupling

M.C. Marchetti, *et al.*, PRL 85, 1104 (2000).

Replace elastic interaction of FLR model by couplings to the local velocity field that are non-local in time.

$$\gamma_0 \dot{u}_i = \sum_{(i,j)} \int_0^t ds C_{i,j}(t-s) [\dot{u}_j(s) - \dot{u}_i(s)] + F + F_i(u_i)$$

Brock Research Group KITP August 19, 2003

41

Modified Swift-Hohenberg Equation

M. Karttunen, *et al.*, PRL 83, 3518 (1999)

Include both amplitude and phase fluctuations.

$$\frac{\partial \psi}{\partial t} + E \frac{\partial \psi}{\partial x} = \left[\varepsilon - \left(q_c^2 + \frac{\partial^2}{\partial x^2} \right)^2 + 4q_c^2 \frac{\partial^2}{\partial y^2} \right] \psi - \psi^3 + \sum_i V_{imp}^i$$

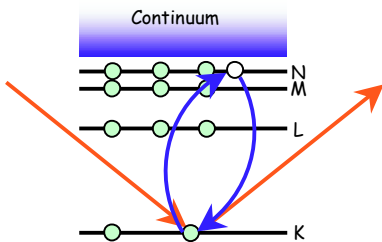
Dislocations proliferate near depinning transition. The dynamical generation of dislocations can make the system *more disordered* above threshold.

Brock Research Group KITP August 19, 2003

42

Resonant Enhancement


Resonant Scattering



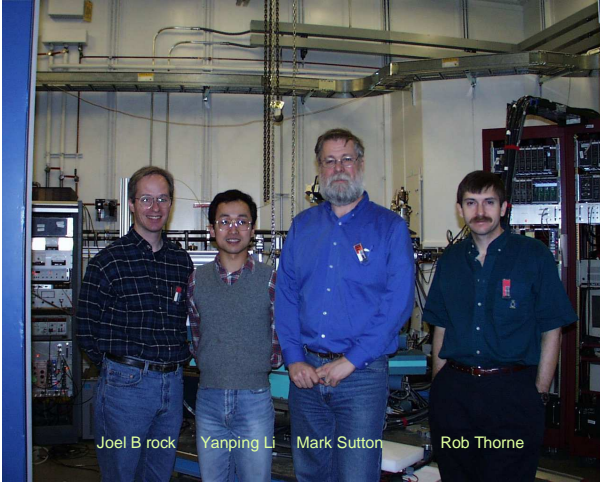
- Use resonant x-ray scattering to sample (diverging) unoccupied density of states of conduction band at $2k_F$.
- Polarization analysis to suppress scattering from LDW

This September at CHESS

Brock Research Group KITP August 19, 2003


 43

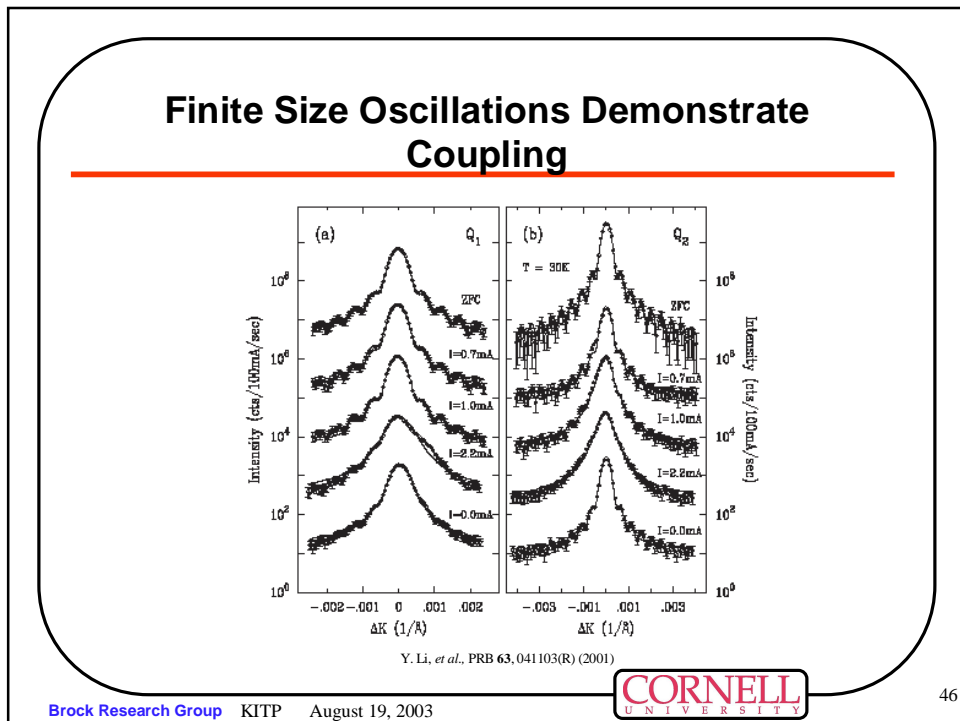
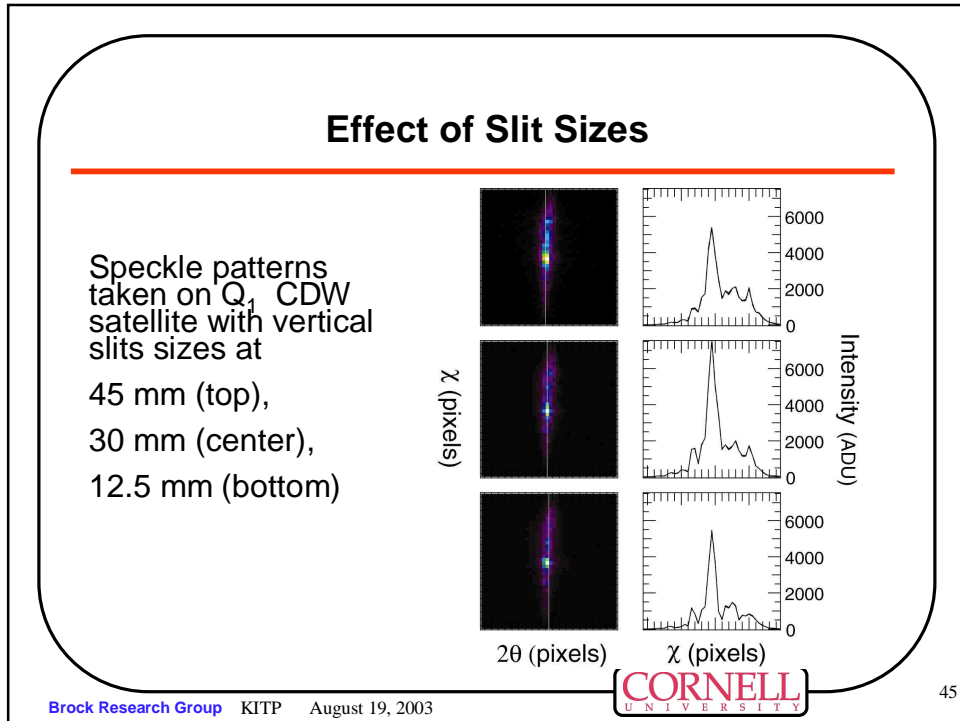
“The Crew”

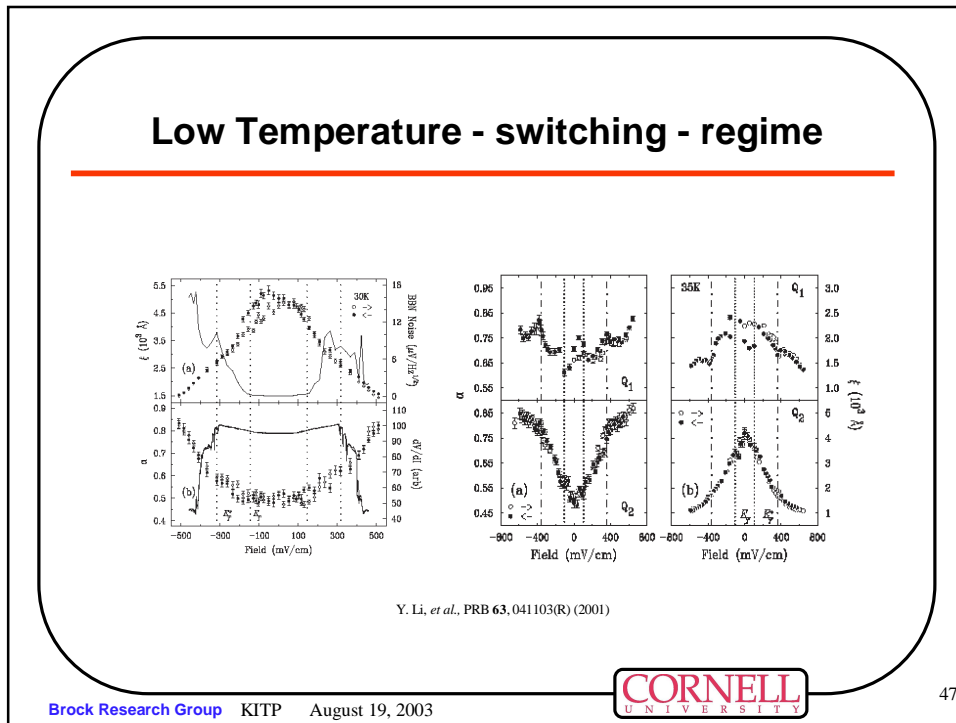


Joel Brock Yanping Li Mark Sutton Rob Thorne

Brock Research Group KITP August 19, 2003

 44





Observations

Non-Ohmic conductivity

- P. Monceau, N.P. Ong, A.M. Portis, A. Meerschaut, and J. Rouxel. "Electric field breakdown of charge-density-wave-induced anomalies in NbSe₃." *Phys. Rev. Lett.*, **37**(10), 602 (1976).
- R.M. Fleming and C.C. Grimes. "Sliding-mode conductivity in NbSe₃: Observation of a threshold electric field and conduction noise." *Phys. Rev. Lett.*, **42**, 1423 (1979).
- H. Matsukawa and H. Takayama. "Numerical study of statics and dynamics of charge-density-waves based on Fukuyama-Lee-Rice model." *Physica B*, **143**, 80 (1986).

Mode-Locking

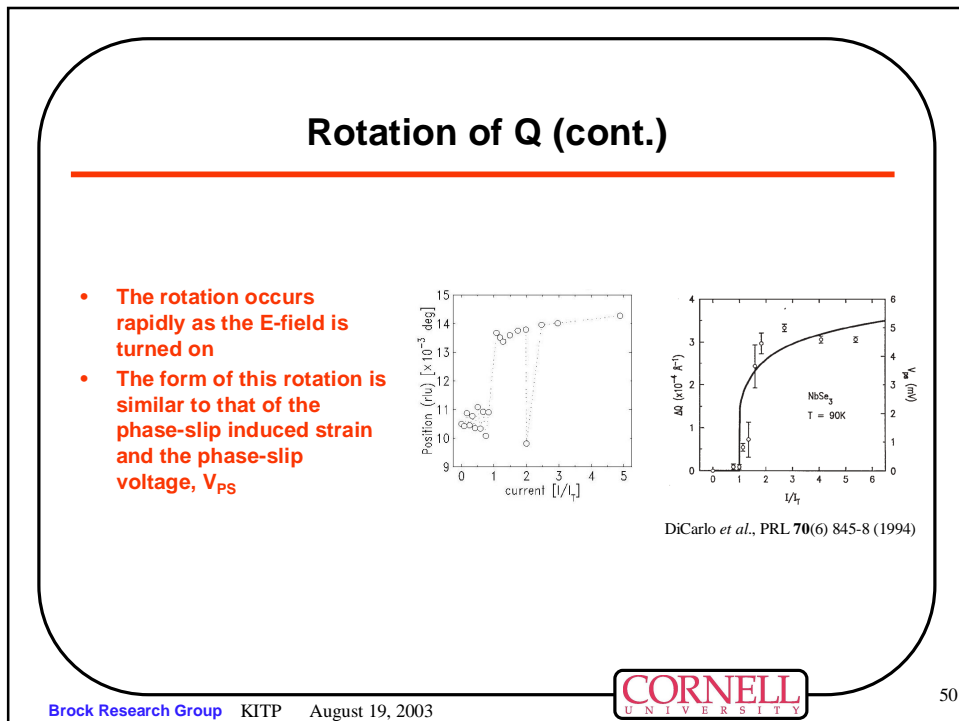
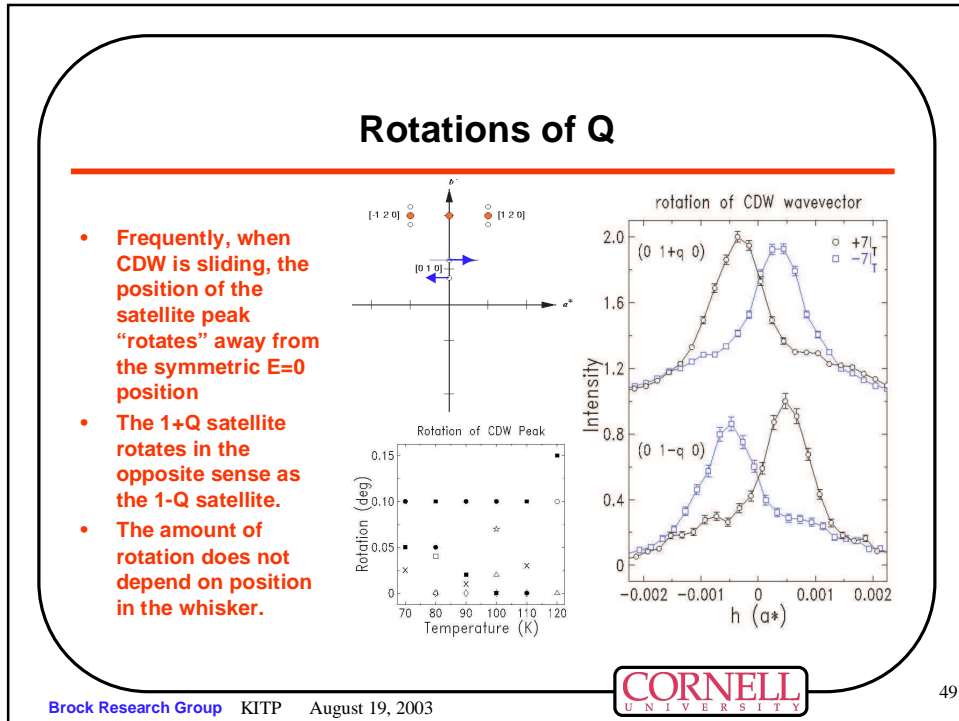
- J.C. Gill. "Transient non-linear phenomena and metastable states of charge-density waves in niobium triselenide." *Solid State Comm.*, **39**, 1203 (1981).
- M. Sherwin and A. Zettl. "Complete charge-density-wave mode locking and freeze-out of fluctuations in NbSe₃." *Phys. Rev. B.*, **32**(8) 5536 (1985).
- S.N. Coppersmith and P.B. Littlewood. "Interference phenomena and mode locking in the model of deformable sliding charge-density waves." *Phys. Rev. Lett.*, **57**(15), 1927 (1986).

Narrow-Band Noise

- R.M. Fleming and C.C. Grimes. "Sliding-mode conductivity in NbSe₃: Observation of a threshold electric field and conduction noise." *Phys. Rev. Lett.*, **42**, 1423 (1979).
- S. Bhattacharya, M.J. Higgins and J.P. Stokes. "Harmonic generation and scaling behavior in sliding-charge-density-wave conductors." *Phys. Rev. Lett.*, **63**(14), 1503 (1989).
- P. Sibanli and P.B. Littlewood. "Critical dynamics of a pinned elastic medium in two and three dimensions: A model for charge-density waves." *Phys. Rev. Lett.*, **64**(11), 1305 (1990).

Brock Research Group KITP August 19, 2003

48



Relationship to Surface Scattering/Growth

	CDWs	Surface Scattering/Growth
Structure Factor	$S(\vec{q}, t) \propto J, (\vec{q} \cdot \vec{u}) ^2 \int d^3\vec{r} e^{i(\vec{G} \pm \vec{Q} - \vec{q}) \cdot \vec{r}} e^{-g(\vec{r}, t)}$	$S(\vec{q}, t) \propto \frac{1}{ (\vec{G} - \vec{q}) \cdot \vec{r} } \int d^3\vec{r} e^{i(\vec{G} - \vec{q}) \cdot \vec{r}} e^{-g(\vec{r}, t)}$
Correlation Function	$g(\vec{r}, t) \equiv \frac{1}{2} \langle [\phi(\vec{r}, t) - \phi(\vec{0}, t)]^2 \rangle$	$g(\vec{r}, t) \equiv \frac{1}{2} \langle [h(\vec{r}, t) - h(\vec{0}, t)]^2 \rangle$
Equation of Motion	$\partial_t \phi = -\Gamma \frac{\delta H_{FLK}}{\delta \phi} + \eta(\vec{r}, t)$	$\partial_t \phi = -\Gamma \frac{\delta H}{\delta \phi} + \eta(\vec{r}, t)$

Brock Research Group KITP August 19, 2003
51

Opening angle of Synchrotron Radiation

On axis
 $\Delta t = (c-v)\Delta t' / c$

Off axis
 $\Delta t = (c-v \cos \alpha)\Delta t' / c$

$$\Delta t \cong \left[1 - \left(1 - \frac{1}{2\gamma^2} \right) \left(1 - \frac{\alpha^2}{2} \right) \right] \Delta t' \cong \left[\frac{1 + (\alpha\gamma)^2}{2\gamma^2} \right] \Delta t'$$

Brock Research Group KITP August 19, 2003
52

Spectrum of Synchrotron Radiation

If T is period of revolution,
 $\Delta t = [\gamma^{-1}/2\pi] T = 1/(\gamma\omega_0)$

Observer "sees" an interval γ^2 shorter
 $\Delta t = 1/(\gamma^3\omega_0)$

Inverse of pulse width gives frequency spread, so high cut-off frequency is
 $\omega_c \equiv (3/2)\gamma^3\omega_0$

$E_c [\text{KeV}] = 0.665 E_e^2[\text{GeV}] B[\text{T}]$

Brock Research Group KITP August 19, 2003
CORNELL UNIVERSITY
53

Sub-Threshold Quenches

- Clearly, phase-slip is occurring and FLR model is not able to describe the dynamics of pinning.
- Quenches from $I < I_T$ should avoid this difficulty.
- Preliminary data suggest that $\mu = 1/2$ for sub-threshold quenches -- consistent with FLR prediction.
- τ appears to be constant -- also consistent with FLR -- but data is not good enough yet.

Brock Research Group KITP August 19, 2003
CORNELL UNIVERSITY
54